Original Investigation

The Role of Different Antioxidant Pathways Like AKT, SIRT-1, NRF2 and HO-1 in Cardiac Damage After Subarachnoid Hemorrhage

Ali Serdar OGUZOGLU[1], Halil ASCI[2], Muhammet Yusuf TEPEBASI[3], Ilter ILHAN[4], Musa CANAN[1], Nilgun SENOL[1], Hakan Murat GOKSEL[1], Ozlem OZMEN[5]

[1]Suleyman Demirel University, Faculty of Medicine, Department of Neurosurgery, Isparta, Türkiye
[2]Suleyman Demirel University, Faculty of Medicine, Department of Pharmacology, Isparta, Türkiye
[3]Suleyman Demirel University, Faculty of Medicine, Department of Genetic, Isparta, Türkiye
[4]Suleyman Demirel University, Faculty of Medicine, Department of Biochemistry, Isparta, Türkiye
[5]Burdur Mehmet Akif Ersoy University, Faculty of Veterinary, Department of Pathology, Burdur, Türkiye

Corresponding author: Nilgun SENOL ✉ drnilgunsenol@yahoo.com

ABSTRACT

AIM: To explore the pathophysiological mechanism of subarachnoid haemorrhage (SAH) using cellular oxidative stress mechanisms and inflammation.

MATERIAL and METHODS: A total of 20 Wistar Albino rats were divided into two groups, namely sham and SAH. On day 0, 0.3 mL of saline in the sham group and 0.3 ml of autologous blood in the SAH group were applied in the cisterna magna of the animals. After sacrification on the 7th day of the procedure, brain, blood and heart tissues were collected.

In different tissues, total antioxidant status (TAS), total oxidant status (TOS), oxidative stress index (OSI), creatin kinase MB (CKMB) and lactate dehydrogenase (LDH) levels were detected biochemically. AKT, sirtuin-1 (SIRT-1), NF-E2–related factor 2 (NRF2), heme oxygenase-1 (HO-1) genes and glutathione peroxidase-4 expression were examined genetically. Moreover, histopathological analyses were conducted both in heart and brain tissues.

RESULTS: Enhanced TOS, OSI levels in all tissues and glial fibrillary acidic protein (GFAP) expressions in brain tissue and NFkβ, IL-6 and Cox-1 expressions in heart tissues; it was observed that levels of TAS in blood and AKT, SIRT-1, NRF2 and HO-1 gene expressions in brain tissue were decreased.

CONCLUSION: In the oxidative stress and inflammation situation that takes place following SAH, AKT, SIRT-1, NRF2 and HO-1 pathways, which are antioxidant mechanisms, are suppressed and GFAP, NFkβ, IL-6, Cox-1 expressions, which trigger inflammation, are enhanced. Treatment of SAH necessitates studies on the inhibition or activation of such pathways.

KEYWORDS: Subaracnoid hemorrhage, Oxidative stress, Inflammation, SIRT-1, NRF-2

ABBREVIATIONS: SAH: Subaracnoid hemorrhage, **TAS:** Total antioxidant status, **TOS:** Total oxidant status, **OSI:** Oxidative stress index, **CKMB:** Creatin kinase MB, **LDH:** Lactate dehydrogenase, **SIRT-1:** Sirtuin-1, **NRF2:** NF-E2–related factor 2, **HO-1:** Heme oxygenase-1, **GFAP:** Glial fibriler asidic protein, **CV:** Cerebral vasospasm, **POM:** Pro-oxidant molecules, **PIC:** Pro-inflammatory cytokines, **NFkβ:** Nuclear factor kappa beta, **IL-6:** Interleukin-6, **Cox-1:** Cyclooxygenase-1, **CSF:** Cerebrospinal fluid, **HE:** hematoxylin-eosin

Ali Serdar OGUZOGLU : 0000-0002-1735-4062
Halil ASCI : 0000-0002-1545-035X
Muhammet Yusuf TEPEBASI : 0000-0002-1087-4874
Ilter ILHAN : 0000-0003-3739-9580
Musa CANAN : 0009-0005-7279-0026
Nilgun SENOL : 0000-0002-1714-3150
Hakan Murat GOKSEL : 0000-0002-9417-0857
Ozlem OZMEN : 0000-0002-1835-1082

INTRODUCTION

Aneurysmal subarachnoid haemorrhage (SAH) has a serious potential for both early and late mortality and morbidity. Late ischaemic cerebral damage due to cerebral vasospasm (CV) results in distant organ dysfunction, which includes the heart and the lungs. This can aggravate clinical conditions due to heart failure, myocardial ischaemia, pulmonary oedema and cardiac dysrhythmia. To manage the aneurysmal SAH cases, the underlying mechanisms of these distant organ malfunctions must be understood.

Secondary to SAH that occurs in the vessels feeding the brain, especially in the region around a ruptured aneurysm, progressive damage with intense oxidative stress and inflammation ensues in the tissues distal to the haemorrhage (7). Damages that take place in other tissues, both secondary to the damage and secondary to the increase in pro-oxidant molecules (POMs) and pro-inflammatory cytokines (PICs) in the blood, increase the permeability of the blood–brain barrier. This situation triggers oxidative stress and inflammation, which leads secondarily to peripheral organ damage such as respiratory failure or cardiac problems (8,14).

PICs and POMs that circulate in the blood reach peripheric organ tissues and activate intracellular signalling mechanisms via their own receptors, which causes the activation of various pathways. Increased expression and activation of genes including nuclear factor kappa beta (NFkβ) within the cell causes the synthesis and release of interleukin-6 (IL-6) and similar cytokines from the cell, which results in the onset of inflammation (10,13). Moreover, cyclooxygenase-1 (Cox-1) enzyme-mediated prostaglandin synthesis increases, contributing to inflammation progression (16).

Inflammation is known to stimulate oxidative stress, which provokes intracellular pathways that involve the NRF2 gene, mediated by the SIRT-1 gene to minimise this oxidative stress (18) (Figure 1).

This study aims to explore the state of the intracellular antioxidant system, which is activated to prevent inflammation, especially oxidative stress, in rats with SAH.

MATERIAL and METHODS

Animals and Ethical Approval

All experiments were carried out following the Animal Research: Reporting in Vivo Experiments (ARRIVE) guidelines 2.0 and were approved by the Suleyman Demirel Univesity, Isparta Committeee on Animal Research (Approval No: 11/05/2023-05/157). A total of 20 adult Wistar albino male rats weighing 300–350 g were used in the experiments. The animals were housed at 21–22°C and 60% ± 5% humidity with a 12-h light:12-h dark cycle and fed with standard commercial feed ad libitum and water during the experiments.

Experimental Protocol

Twenty rats were divided into two groups as follows:

1. Sham Group (n=10): In this group, only 0.3 mL of physiological saline solution was applied to the cisterna magna of the animals.
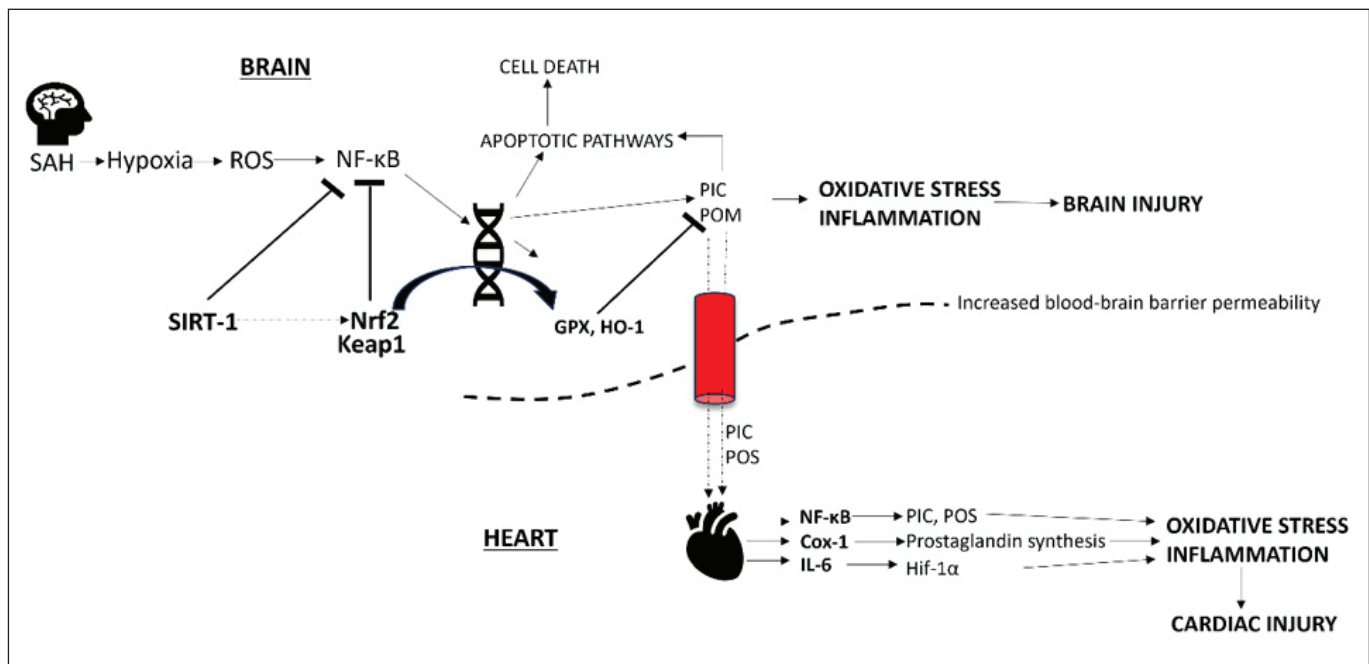

Figure 1: Possible physiopathogenesis of SAH induced cardiac toxicity via inflammation. **SAH:** Subarachnoid hemorrhage, **ROS:** Reactive oxygen species, **SIRT1 1:** Sirtuin 1, **AKT1:** serine/threonine-protein kinase 1, **NRF2:** NF-E2–related factor 2, **KEAP1:** Kelch-like ECH-associated protein 1, **HO-1:** Heme Oxygenase 1, **GPX4:** Glutathione Peroxidase 4, **PIC:** Pro-inflammatory cytokines, **POS:** Pro-oxidant molecules, **IL-6:** Interleukin-6, **Hif-1α:** Hypoxia inducible factor-alpha, **NFkβ:** Nuclear factor kappa beta, **Cox-1:** Cyclooxygenase-1.

2. SAH Group (*n=10*): After 0.3 mL of cerebrospinal fluid (CSF) aspirated, 0.3 mL of autologous blood obtained from the tail artery was injected into the cisterna magna over 2 min (5).

All animals were sacrificed on the morning of the seventh day under 80–100-mg/kg ketamine (Keta-control, Doga Ilac, Turkey)/8–10-mg/kg xylazine (Xylazinbio %2, Bioveta, Czech Republic) anaesthesia via exsanguination. Blood samples were taken from the vena cava inferior, and brain-heart tissue samples were dissected after decapitation and abdominal incision, respectively. Brain and heart tissues were divided into two portions; half of the tissues were placed in 10% formaldehyde for histopathological and immunohistochemical analysis, and the other half was placed at −80° for biochemical analysis.

Histopathological Evaluation

During the necropsy, brain and heart sample tissues were collected and fixed in 10% buffered formalin for histopathological analysis. After routine processing, the tissues with a fully mechanised tissue processor, 5-µm-thick pieces of the paraffin blocks were cut using fully automatic rotary microtomes (Leica RM2155, Leica Microsystems, Wetzlar, Germany). Deparaffinisation, rehydration with ethanol graded in decreasing quantities, staining with haematoxylin–eosin, cleaning in xylene and covering the sections were the next steps. The histological changes were assessed under a light microscope. Histopathological changes scored on a four-point scale: 0) none, 1) mild, 2) moderate and 3) severe damage.

Immunohistochemical Examinations

Brain sections were stained with GFAP, and heart sections, with Cox-1, IL-6 and NFkβ. Sections taken onto polylysine-coated slides were immunostained for GFAP (anti-GFAP antibody (ab7260), Hif-1α (anti-HIF-1 alpha antibody [mgc3] (ab16066)), NFkβ (anti-NF-kβ p65 antibody (ab16502)): Cox-1 (anti-COX1/cyclooxygenase 1 antibody [EPR5866] (ab109025) and IL-6 (anti-IL-6R antibody [EPR26370-132] (BSA and azide free) (ab300582)) using the streptavidin–biotin technique. We purchased primary and secondary antibodies from Abcam (Cambridge, UK), and primary antibodies were used as 1/100 dilution. After a 60-min incubation period with primary antibody, sections were immunohistochemically stained using biotinylated secondary antibodies and streptavidin–alkaline phosphatase conjugate. EXPOSE Mouse and Rabbit Specific HRP/DAB Detection IHC kit (ab80436) was utilised as the secondary antibody, and diaminobenzidine was used as the chromogen (DAB). For the negative controls, the primary antiserum step was swapped out for the dilution solution. For each marker, all slides were analysed for immunopositivity. The number of positive cells was determined in one high-power field. For this purpose, 100 cells were counted under 40X magnification for each rat using ImageJ (National Institutes of Health, Bethesda MD). The Database Manual Cell Sens Life Science Imaging Software System (Olympus Co., Tokyo, Japan) was employed for microphotography.

Measurement of Oxidative Stress Parameters in the Brain, Blood and Heart Tissues

Heart and brain tissues of rats were homogenised with the Ultra Turrax Janke & Kunkel T-25 homogeniser (IKA® Werke, Germany). After that homogenised tissues were centrifuged at 10000 rpm for 10 min. Using a modified Erel method, the serum TAS, TOS and OSI values were measured spectrophotometrically (3). The TAS and TOS results in the serum were expressed in µmol Trolox Eq/L and µmol H_2O_2 Eq/L, respectively. The TAS and TOS results for the tissues were expressed by dividing them by the protein value (12). The OSI was calculated using the formula OSI = (TOS/TAS) × 100 (4).

The collected rats' blood was centrifuged at 3000 RPM for 15 min, and serum CK-MB levels and LDH levels were measured spectrophotometrically with a Beckman Coulter AU5800 autoanalyzer (Beckman Coulter, USA).

Reverse Transcription–Polymerase Chain Reaction (RT-qPCR)

Using the GeneAll RiboEx (TM) RNA Isolation Kit (Cat No: 301–001) and according to the manufacturer's instructions, RNA was extracted from homogenised lung tissues (GeneAll Biotechnology, Seoul, Korea). To measure the quantity and purity of the RNAs that were collected, a BioSpec-nano NanoDrop UV–Vis spectrophotometer (UV-2600, Shimadzu Ltd. Kyoto, Japan) instrument was employed. cDNA synthesis was conducted using the A.B.T.™ cDNA Synthesis Kit (Cat No: C03-01–05) from Atlas Biotechnology in Turkey in accordance with the instructions. For cDNA synthesis, 1 µg of RNA was utilised. Using the Primer-BLAST tool (NCBI website), specific mRNA sequences were found, and potential primer sequences were then tested. In Table I, the primers' sequences used, accession numbers and product size of the genes are provided. A.B.T.™ SYBR Master Mix (Atlas Biotechnology, Turkey) (Cat No: Q04-01–05) was employed to quantify the expression levels of genes in a Biorad CFX96 real-time PCR equipment (CA, USA). In the research, the ACTB gene was utilised as the housekeeping gene in the heart tissue, and the rn18s gene was employed as the housekeeping gene in brain tissue. The reaction mixture was prepared based on the manufacturer's protocol to a final volume of 20 µL. The resultant reaction mixture was put into real-time qPCR equipment with a thermal cycling setup according to the manufacturer's protocol for the kit, and each sample was investigated in three replications. The PCR protocol was applied as one cycle with an initial denaturation at 95°C for 300 s and 40 cycles with denaturation at 95°C for 15 s, annealing/extension at 55°C for 30 s. Relative mRNA levels were calculated by applying the $2^{-\Delta\Delta Ct}$ formula to normalise the results (11).

Statistical Analysis

Variables were presented as mean ± standard deviations. Independent *t*-tests were employed to compare biochemical and genetic scores between the two groups. Statistical calculations were carried out using the GraphPad Prism 8.0 program pack (GraphPad Software, Inc., USA); p<0.05 was set as the value for significance.

RESULTS

Biochemical Findings

TOS, TAS and OSI values of brain, blood and heart tissues

TOS values measured in the brain, blood and heart tissues were found to be significantly higher than in the control group (p=0.02, p=0.001 and p=0.007; respectively). Furthermore, OSI values were found to be significantly higher in the aforementioned tissues than in those of the control group (p=0.001, p=0.04 and p=0.003; respectively). When TAS values were examined, there was a statistically significant decrease in the brain and blood when compared to the control group (p=0.007 and p=0.02), although there was only a modest decrease in the heart tissues (p=0.62) (Figure 2).

GPX4 values in heart tissues and cardiac biochemical markers in blood tissues

The amount of antioxidant GPX4 in the heart tissues decreased in the SAH group when compared to the control group (p = 0.06), but it was not statistically significant.

Although an increase in CKMB levels (p=0.38) and a decrease in LDH levels (p=0.85), which are indicators of cardiac damage, were observed in the blood, there was no statistical significance detected (Figure 3).
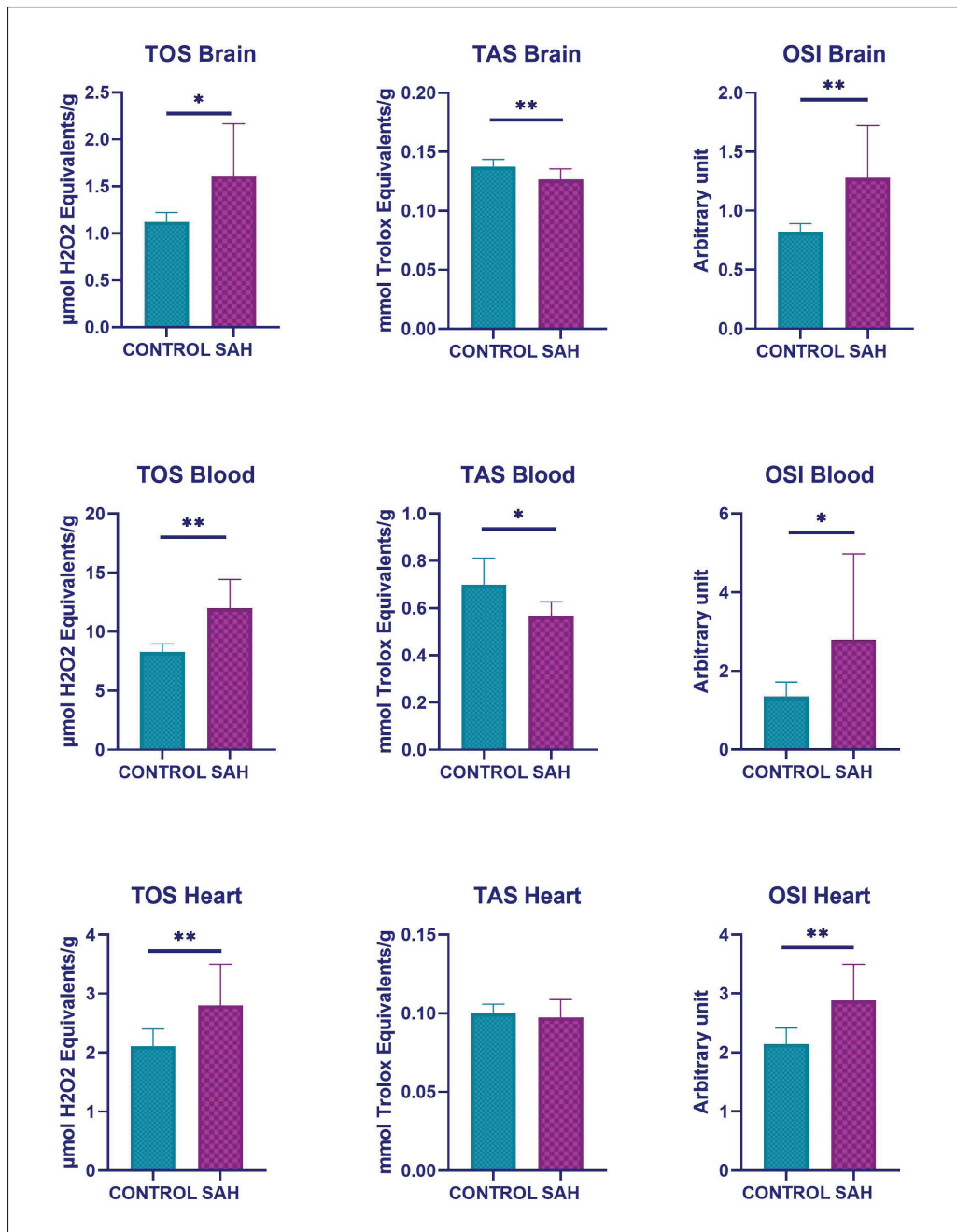

Figure 2: Oxidative stress parameters in brain, blood and heart tissues
Values are presented as means ± standard deviation. Nonparametric t test was used. **SAH:** Subaracnoidal hemorrhage, **TAS:** Total antioxidant status, **TOS:** Total oxidant status, **OSI:** Oxidative stress index, ***:** SAH vs control group. *p≤0.05, **p≤0.01, ***p≤0.001.

Histopathological Findings

At the microscopical examinations of brains, no lesions were observed in the control group. Nevertheless, SAH caused inflammatory cell infiltrations and oedema at the meninges. Additionally, gliosis, varying degrees of hyperemia and neuronal degeneration characterised by neuron shrinkage in the brain cortex ($p \leq 0.001$), cerebellum ($p \leq 0.001$) and hippocampus ($p \leq 0.025$) were commonly observed in the SAH group (Figure 4).

Additionally, severe hyperemia, haemorrhage, oedema, myocardial damage and slight inflammatory cell infiltrations were observed in the SAH group, whereas normal cardiac histology was noted in the sham group (Figure 5).

Table I: Primary Sequences, Product Size and Accession Numbers of Genes

Genes	Primary sequence	Product size	Accession number
ACTB (HouseKeeping)	F: CCCGCGAGTACAACCTTCTT	481 bp	NM_031144.3
	R: AACACAGCCTGGATGGCTAC		
Rn18s (HouseKeeping)	F: CTCTAGATAACCTCGGGCCG	209 bp	NR_046237.2
	R: GTCGGGAGTGGGTAATTTGC		
SIRT-1	F: GGTAGTTCCTCGGTGTCCT	152 bp	NM_001414959.1
	R: ACCCAATAACAATGAGGAGGTC		
AKT1	F: AGTCCCCACTCAACAACTTCT	119 bp	XM_006240631.3
	R: GAAGGTGCGCTCAATGACTG		
NRF2	F: GCCTTCCTCTGCTGCCATTAGTC	126 bp	NM_001399173.1
	R: TCATTGAACTCCACCGTGCCTTC		
KEAP-1	F: TGGTTCCTGCAACTTGGTGA	372 bp	NM_057152.2
	R: CTATGTGTCCCACAAGGGAGC		
HO-1	F: AGCCTGGTTCAAGATACTACCTC	240 bp	XM_039097470.1
	R: AGGCCCAAGAAAAGAGAGCC		
GPX4	F: CATTGGTCGGCTGCGTGA	276 bp	NM_017165.4
	R: GGTTTTGCCTCATTGCGAGG		

*F: Forward, **R:** Reverse, **ACTB:** Actin Beta, **Rn18s:** 18S ribosomal RNA, **SIRT-1:** Sirtuin-1, **AKT1:** Serine/threonine-protein kinase 1, **NRF2:** NF-E2–related factor 2, **KEAP-1:** Kelch-like ECH-associated protein-1, **HO-1:** Heme Oxygenase 1, **GPX4:** Glutathione Peroxidase 4.*
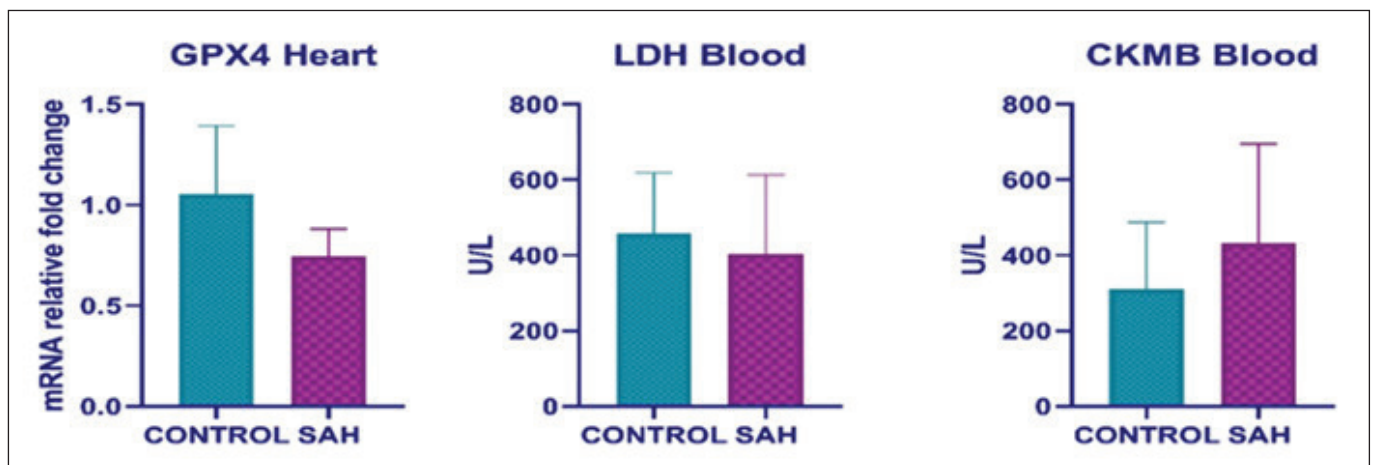

Figure 3: mRNA relative fold change of GPX4 in heart and biochemical markers of heart in blood tissue. Values are presented as means ± standard deviation. Nonparametric t test was used. **SAH:** Subaracnoidal hemorrhage, **GPX4:** Glutathione peroxidase-4, **LDH:** Lactate dehydrogenase, **CKMB:** Creatin kinase MB.
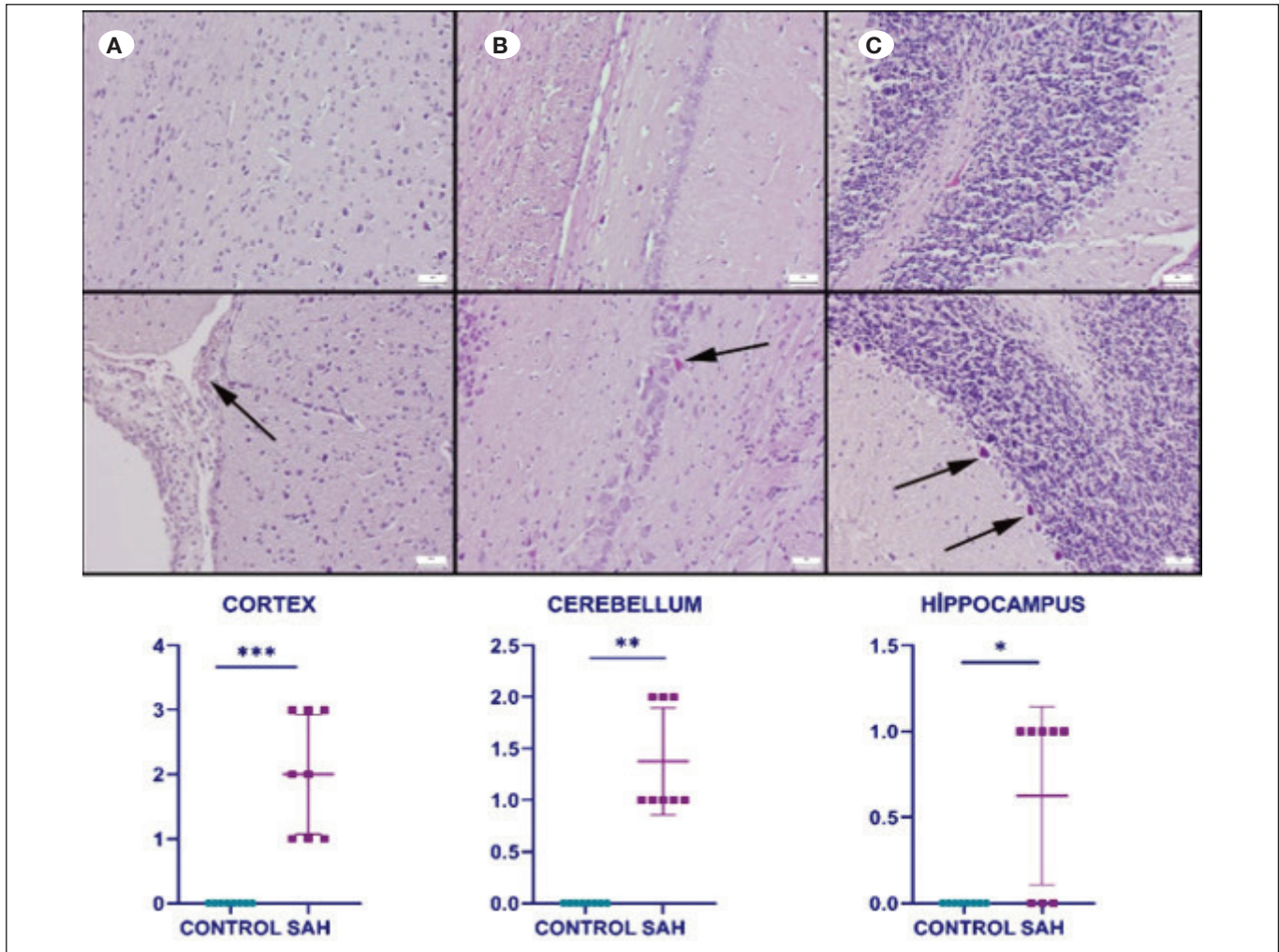
Figure 4: Histopathological findings in control (upper row) and SAH (below row) between the groups. **A)** Normal brain histology in control group and inflammatory reaction, hemorrhage and edema (arrow) brain in SAH group, **B)** normal hippocampus architecture in control group and degenerative neurons (arrow) in SAH group, **C)** normal cerebellum histology in control group and shrinkage in Purkinje cells (arrows) in SAH group, HE, scale bars=50μm.
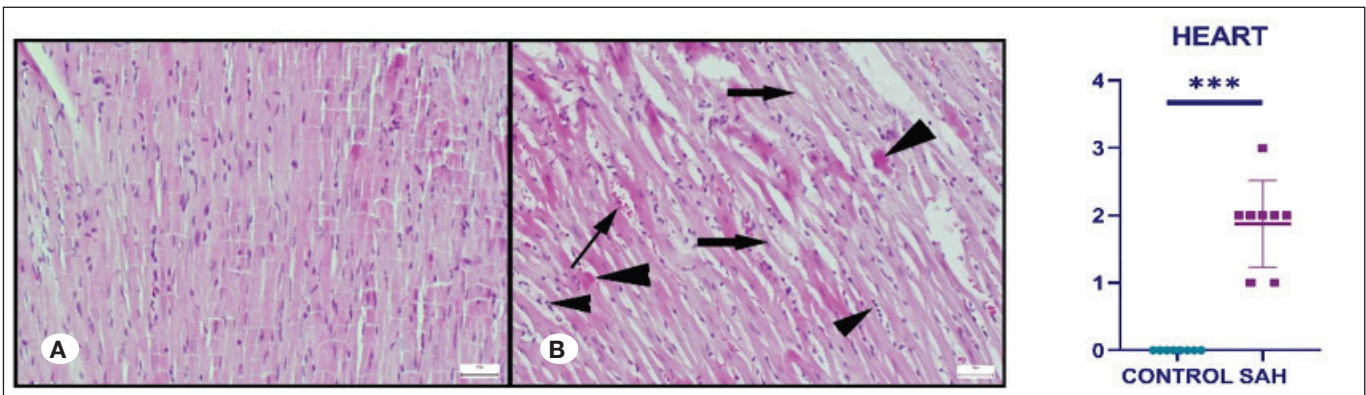

Figure 5: Representative histopathological microphotograph of hearts. **A)** Normal heart tissue architecture in control group, **B)** hemorrhage (thin arrow), edema (thick arrows), inflammatory cell infiltrations (thin arrow heads) and myocardial cell damage (thick arrow heads), HE, scale bars=50μm.

Immunohistochemical examination of the brain, cerebellum and hippocampus sections showed that the SAH group's GFAP expressions were higher than those of the control group (p<0.001 for all, Figure 6).

In the sections stained with immunohistochemical methods, the heart in the SAH group had increased expressions of Cox-1, IL-6 and NFkβ (p<0.001 for all). Expressions were frequently concentrated in the myocardial cells (Figure 7).

Genetic Results

RT-qPCR results

In brain tissues, AKT, SIRT-1, NRF2, KEAP-1 and HO-1 gene expressions were significantly decreased in the SAH group (p≤0.001, p=0.001, p=0.001, p≤0.001 and p≤0.001, respectively). Parallel to these findings, all of these parameters decreased significantly in heart tissues (p=0.004, p=0.006, p=0.026, p=0.03 and p=0.033, respectively), and the decreases in cardiac tissue were higher than those in brain tissue (Figure 8).

■ DISCUSSION

In this study, several mechanisms, especially oxidative stress and inflammation, which may have a role in the pathogenesis of cardiac damage in the SAH model established in rats, were examined. The results of the study revealed that oxidative stress indicators increased in the brain, blood and heart tissues. Additionally, AKT, SIRT-1, NRF2 and HO-1 pathways, which are intracellular mechanisms that play a role in antioxidant activity in brain and heart tissues, were suppressed. Increased inflammatory parameters, including NFkβ, IL-6 and Cox-1 expressions, promote brain tissue damage.

In SAH, which has a very aggressive and progressive clinical course, the tissue damage mechanisms are activated by the hypoxic environment occurring distal to the scene of the incident, secondary to both bleeding itself and CV caused by some substances released from blood elements extravasated due to bleeding (15). PIS and POMs taking place in the vessels distal to bleeding can directly cause damage to the distal
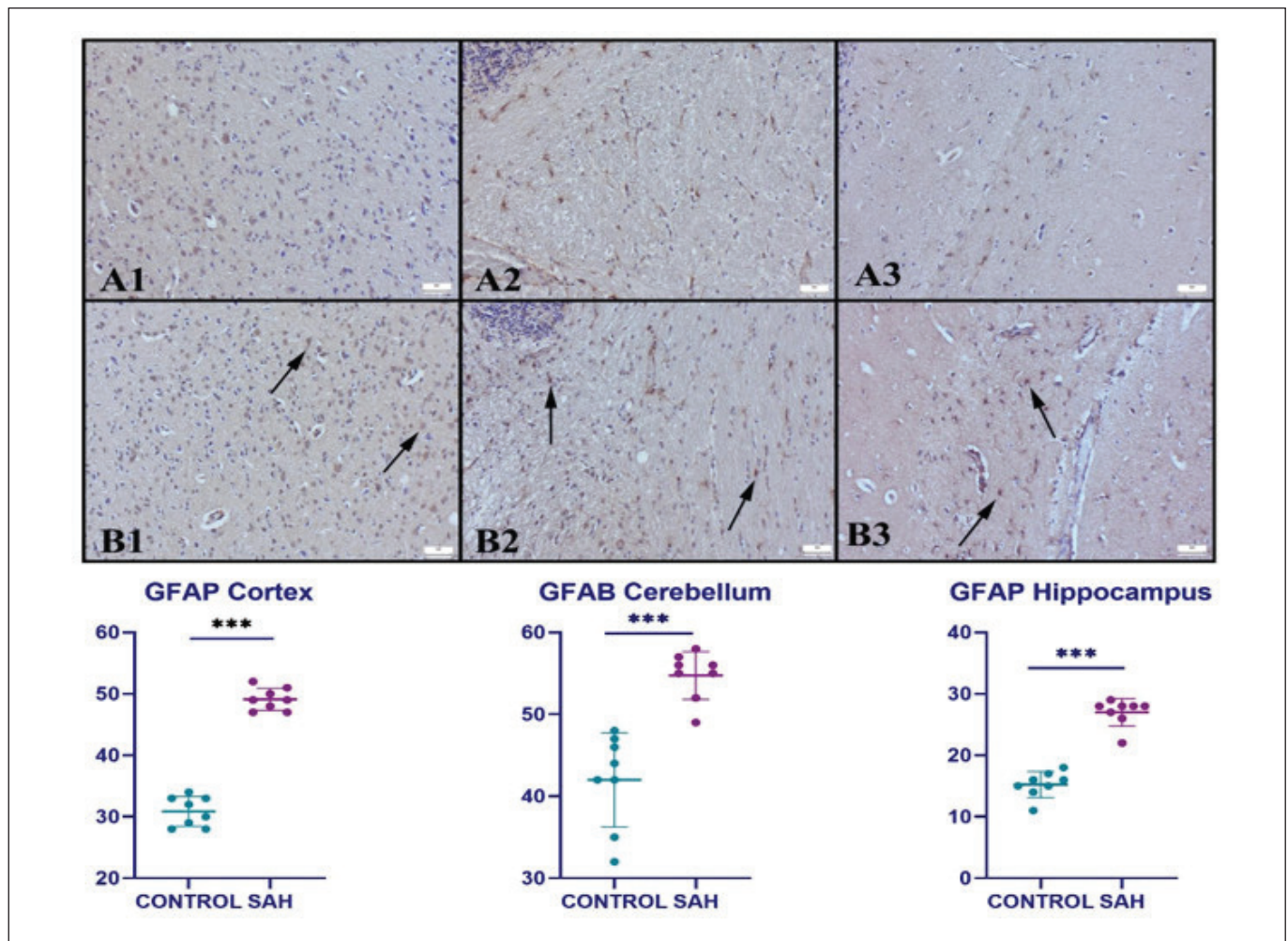

Figure 6: GFAP immunoexpressions of the brain tissues. Normal expression in cerebral cortex **(A1)**, cerebellum **(A2)** and hippocampus **(A3)** in control group, increased GFAP expressions in neorons of cerebral cortex **(B1)**, cerebellum **(B2)** and hippocampus **(B3)** in SAH groups (arrows), streptavidin biotin peroxidase method, Scale bars=50µm.
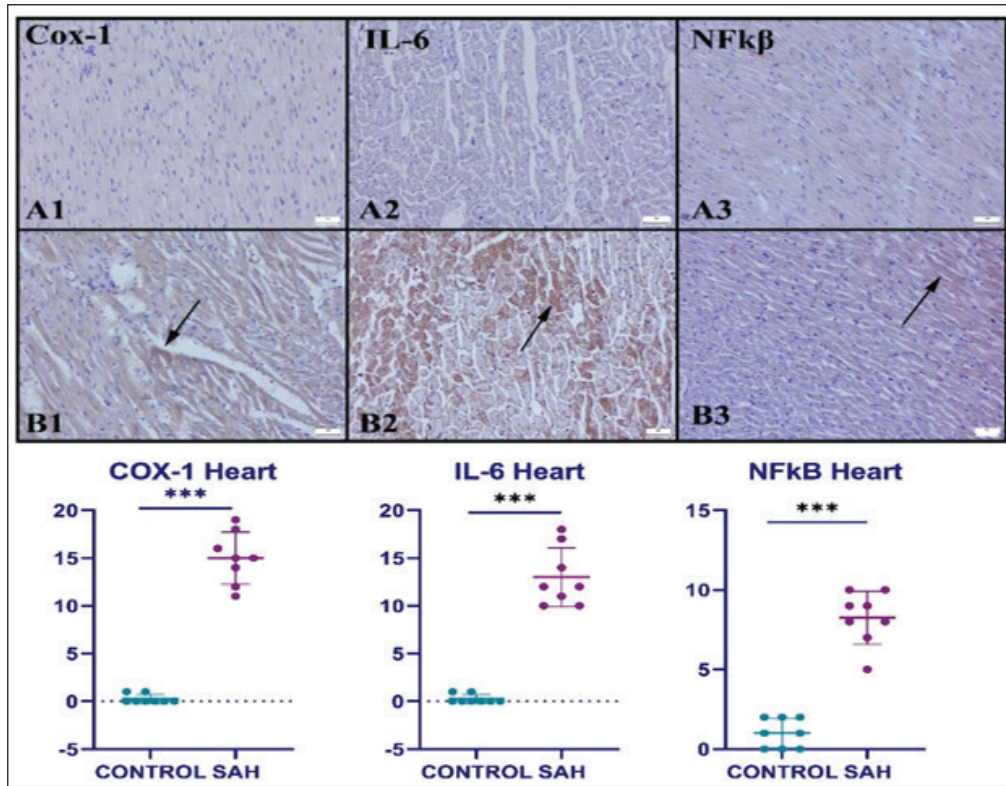
Figure 7: Cox-1, IL-6 and NFkβ immunoexpressions of the hearts. Cox-1 (A1), IL-6 (A2) and NFkβ (A3) immunostaining of sham and increased Cox-1 (B1), IL-6 (B2) and NFkβ (B3) immunostaining of SAH groups (arrows), streptavidin biotin peroxidase method, Scale bars=50μm.
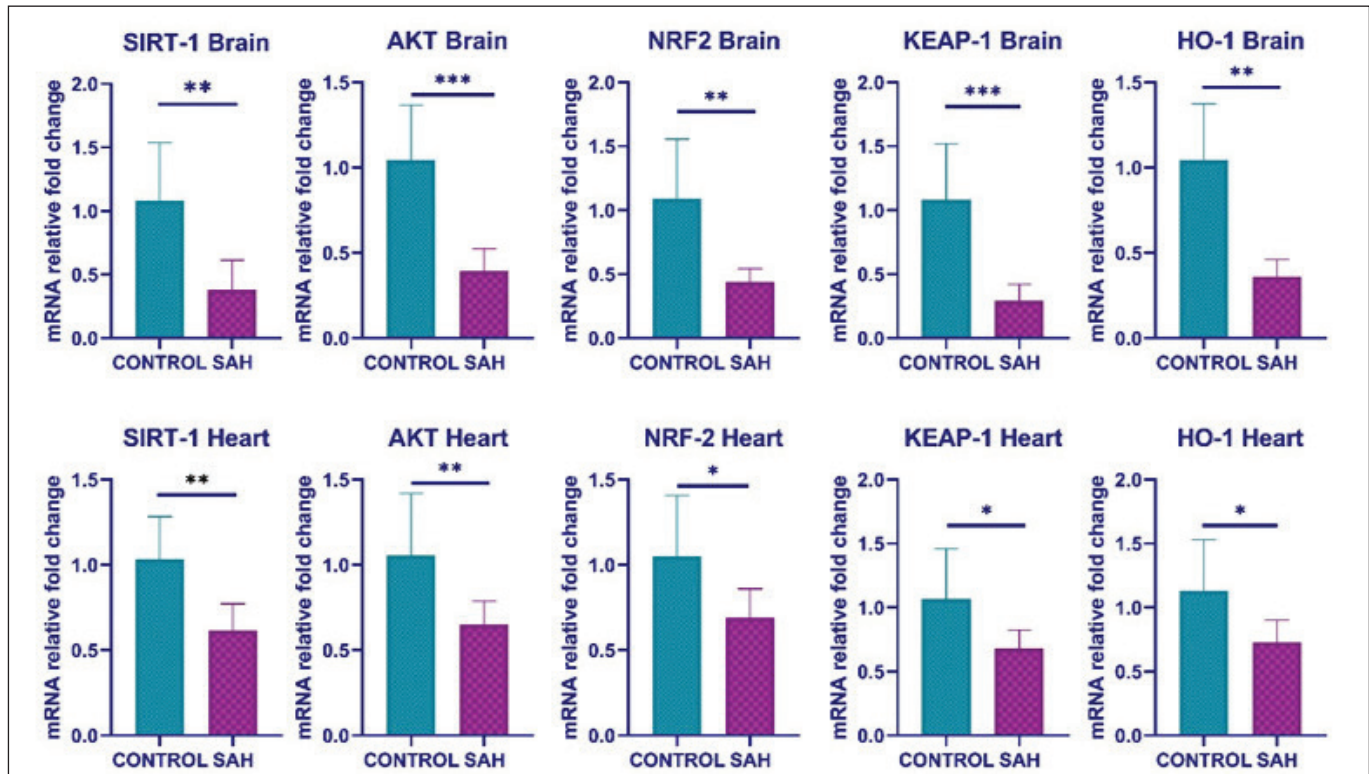

Figure 8: mRNA relative fold changes of SIRT-1, AKT, NRF2, KEAP-1 and HO-1 genes in brain and heart tissues. Values are presented as means ± standard deviation. Nonparametric t test was used. **SAH:** Subaracnoidal hemorrhage, **SIRT-1 1:** Sirtuin-1, **AKT1:** serine/threonine-protein kinase 1, **NRF2:** NF-E2–related factor 2, **KEAP-1:** Kelch-like ECH-associated protein 1, **HO-1:** Heme Oxygenase 1, **GPX4:** Glutathione Peroxidase-4.

brain tissue through their own receptors and can also cause the damage to spread to peripheral tissues by increasing the permeability of the blood–brain barrier (17). PIS and POMs circulating in vascular structures outside the brain can trigger damage in peripheral structures, especially the heart, similar to that in brain tissue (14).

Several intracellular pathways can be activated when damage takes place at the tissue level. For instance, Hif-1α levels, whose expression increases by binding to the cell receptors of IL-6, which is an acute phase protein and whose levels increase in rapidly developing situations, support the inflammatory response by increasing the expressions of VEGF and eNOS, which are hypoxia-induced physiopathological responses (1,10,13). Additionally, the increase in the expression and activation of genes that have a central role within the cell, such as NFkβ, can increase the development of PIS and POM mediated by the cell nucleus. These new stimuli taking place at the tissue level can also affect healthy cells in the environment and contribute to the progressive course of damage (2). Aside from these mechanisms mentioned, prostaglandins, whose synthesis increases through arachidonic acid metabolism, also support the inflammatory situation (16).

Given that this study is a SAH model, cerebral tissue damage is principal, whereas the damage that occurs in the blood and other peripheral tissues is less severe than in the brain. In clinical practice, secondary damage to SAH occurring in the highly vascularised lung and heart tissues, can cause an increase in organ-specific biomarkers, and even death occurs due to peripheral organ damage (9).

Protective mechanisms come into play at the cellular level in brain tissue and other organs against the above-mentioned damages. Normally, damage and these protective mechanisms are in balance, or the protective systems are more dominant, which can prevent the progression of the lesion or cause it to regress (6). Some basic intracellular mechanisms ensure the increase in anti-inflammatory substances including IL-10 and IL-4, which the body produces endogenously, and antioxidant substances such as GPX4 and catalase (19). The increase in SIRT-1 gene levels mediated by AKT, one of the most important of these, may cause the synthesis of antioxidant substances such as HO-1 and GPX4 mediated by the NRF2 gene, which will play a role in defense against damage (19,20). Normally, by increasing a certain amount of antioxidants, minor damage can be minimised. Conversely, if the damage is severe, using the specified antioxidants more than necessary for this minimisation may cause an early insufficiency in their levels. In this study, the decrease in SIRT-1 gene expression levels in brain tissue where the damage was most severe, and the secondary expression of other genes revealed an insufficient response to the brain tissue damage. The effect of the mentioned mechanisms is supported by the increase in TOS and OSI levels and the decrease in TAS levels, which collectively indicate the damage caused by oxidative stress detected in brain tissue as a final response to the suppression of these cellular mechanisms.

Due to the increase in permeability in the blood–brain barrier, PICs and POMs that take place in the injured brain tissue are released into the blood or formed directly in the blood that passes through the peripheral circulation (17). Observation of an increase in POM levels in the blood, although not as much as in brain tissue, as well as a decrease in the amount of antioxidant substances, will be meaningful in establishing the connection between brain damage and cardiac damage. The increase in TOS and OSI levels and the decrease in TAS levels in the blood, which we have revealed in this study, may indicate that oxidative stress is triggered in the blood. There has not been a sufficient cellular-level investigation in the literature regarding the fact that these POMs circulating in the blood can cause damage by stimulating intracellular mechanisms when they reach the heart tissue, as in the brain tissue. Since oxidative stress triggers inflammation, TOS, TAS, OSI and Cox-1, NFkβ and IL-6 expressions, which will be checked in the occurrence of damage to the heart, will indicate both pathological events. The increase in Cox-1, NFkβ and IL-6 expressions shown by immunohistochemical analyses in the heart indicates that inflammation has occurred, and increased TOS and OSI values indicate oxidative stress. Here, the significant increase in oxidant molecules in the heart tissues and the observation of a non-significant decrease in antioxidant TAS and GPX4 levels to balance this increase can be interpreted as the late onset of heart pathology secondary to brain damage. The antioxidant system used to suppress this oxidative stress, which occurs at lower levels in the heart tissues, may further decrease over time.

In this study, to show the development of the mentioned cardiac damage, the same markers in the brain tissue samples were also examined in the heart tissue samples. The fact that the significant decreases in AKT, SIRT-1, NRF-2, KEAP-1 and HO-1 levels and the non-significant damage in GPX4 and TAS levels are less than in the brain tissue indicates that oxidative stress is milder in the heart.

The findings of this study on changes in CKMB and LDH levels after experimental SAH, which are the most important clinical indicators of damage to the heart tissues, revealed insignificant changes, which also supports this situation (9). In other words, intracellular mechanisms that are related to antioxidant defence, which are examined at the tissue level via a detailed analysis such as PCR, were activated; consequently, damage to the heart tissue occurred at the molecular level, and the increase in cardiac damage indicators did not occur in the blood.

■ CONCLUSION

Oxidative stress and inflammation develop in the blood and heart tissue due to increased permeabilirty of the blood-brain barrier following SAH injury. To prevent oxidative stress from occurring in brain and heart tissues, the expressions of AKT, SIRT-1, NRF-2, KEAP-1 and HO-1, which are important intracellular genes in antioxidant defence, were decreased. This depletion in cardiac tissues and the parallel development of inflammation may play a role in cardiac damage secondary to SAH. Elucidating other intracellular pathways in which these mechanisms are associated with advanced molecular methods will contribute to the selection of treatment agents.

AUTHORSHIP CONTRIBUTION

Study conception and design: ASO, HA

Data collection: ASO, HA, MC, OO

Analysis and interpretation of results: HA, MYT, II

Draft manuscript preparation: ASO, HA, NS

Critical revision of the article: ASO, HA, NS, HMG

Other (study supervision, fundings, materials, etc...): HA, MC, MYT, II, OO

All authors (ASO, HA, MYT, II, MC, NS, HMG, OO) reviewed the results and approved the final version of the manuscript.

■ REFERENCES

1. Duan MX, Zhou H, Wu QQ, Liu C, Xiao Y, Deng W, Tang QZ: Andrographolide protects against HG-induced inflammation, apoptosis, migration, and impairment of angiogenesis via PI3K/AKT-eNOS Signalling in HUVECs. Mediators Inflamm 2019: 6168340, 2019. https://doi.org/10.1155/2019/6168340

2. El-Shitany NA, Eid BG: Icariin modulates carrageenan-induced acute inflammation through HO-1/Nrf2 and NF-kB signaling pathways. Biomed Pharmacother 120:109567, 2019. https://doi.org/10.1016/j.biopha.2019.109567

3. Erel O: A novel automated direct measurement method for total antioxidant capacity using a new generation, more stable ABTS radical cation. Clin Biochem 37:277-285, 2004. https://doi.org/10.1016/j.clinbiochem.2003.11.015

4. Erel O: A new automated colorimetric method for measuring total oxidant status. Clin Biochem 38:1103-1111, 2005. https://doi.org/10.1016/j.clinbiochem.2005.08.008

5. Han SM, Wan H, Kudo G, Foltz WD, Vines DC, Green DE, Zoerle T, Tariq A, Brathwaite S, D'Abbondanza J, Ai J, Macdonald RL: Molecular alterations in the hippocampus after experimental subarachnoid hemorrhage. Journal of cerebral blood flow and metabolism. J Cereb Blood Flow Metab 34 108-117, 2014. https://doi.org/10.1038/jcbfm.2013.170

6. Laskowitz DT, Kolls BJ: Neuroprotection in subarachnoid hemorrhage. Stroke 41 Suppl 10: S79-S84, 2010. https://doi.org/10.1161/STROKEAHA.110.595090

7. Lauzier DC, Jayaraman K, Yuan JY, Diwan D, Vellimana AK, Osbun JW, Chatterjee AR, Athiraman U, Dhar R, Zipfel GJ: Early brain injury after subarachnoid hemorrhage: Incidence and mechanisms. Stroke 54:1426-1440, 2023. https://doi.org/10.1161/STROKEAHA.122.040072

8. Li R, Yuan Q, Su Y, Chopp M, Yan T, Chen J: Immune response mediates the cardiac damage after subarachnoid hemorrhage. Exp Neurol 323:113093, 2020. https://doi.org/10.1016/j.expneurol.2019.113093

9. Li W, Leng Y, Xiong Y, Xia Z: Ferroptosis is involved in diabetes myocardial ischemia/reperfusion injury through endoplasmic reticulum stress. DNA Cell Biol 39:210-225, 2020. https://doi.org/10.1089/dna.2019.5097

10. Liu M, Jayaraman K, Mehla J, Diwan D, Nelson JW, Hussein AE, Vellimana AK, Abu-Amer Y, Zipfel GJ, Athiraman U: Isoflurane conditioning provides protection against subarachnoid hemorrhage induced delayed cerebral ischemia through NF-kB inhibition. Biomedicines 11:1163, 2023. https://doi.org/10.3390/biomedicines11041163

11. Livak KJ, Schmittgen TD: Analysis of relative gene expression data using real-time quantitative PCR and the 2(-Delta Delta C(T)) method. Methods 25:402-408, 2001. https://doi.org/10.1006/meth.2001.1262

12. Lowry OH, Rosebrough NJ, Farr AL, Randall RJ: Protein measurement with the Folin phenol reagent. J Biol Chem 193:265-275, 1951. https://doi.org/10.1016/S0021-9258(19)52451-6

13. Lucke-Wold B, Hosaka K, Dodd W, Motwani K, Laurent D, Martinez M, Hoh B: Interleukin-6: Important mediator of vasospasm following subarachnoid hemorrhage. Curr Neurovasc Res 18:364-369, 2021. https://doi.org/10.2174/1567202618666211104122408

14. Mazeraud A, Robba C, Rebora P, Iaquaniello C, Vargiolu A, Rass V, Bogossian EG, Helbok R, Taccone FS, Citerio G: Acute distress respiratory syndrome after subarachnoid hemorrhage: Incidence and impact on the outcome in a large multicenter, retrospective cohort. Neurocrit Care 34:1000-1008, 2021. https://doi.org/10.1007/s12028-020-01115-x

15. Naraoka M, Matsuda N, Shimamura N, Asano K, Ohkuma H: The role of arterioles and the microcirculation in the development of vasospasm after aneurysmal SAH. BioMed Res Int 2014:253746, 2014. https://doi.org/10.1155/2014/253746

16. Simon LS: Role and regulation of cyclooxygenase-2 during inflammation. Am J Med 106:37S-42S, 1999. https://doi.org/10.1016/S0002-9343(99)00115-1

17. Wang XY, Wu F, Zhan RY, Zhou HJ: Inflammatory role of microglia in brain injury caused by subarachnoid hemorrhage. Front Cell Neurosc 16:956185, 2022. https://doi.org/10.3389/fncel.2022.956185

18. Xu C, Song Y, Wang Z, Jiang J, Piao Y, Li L, Jin S, Li L, Zhu L, Yan G: Pterostilbene suppresses oxidative stress and allergic airway inflammation through AMPK/Sirt1 and Nrf2/HO-1 pathways. Immun Inflamm Dis 9:1406-1417, 2021. https://doi.org/10.1002/iid3.490

19. Xu L, Gao Y, Hu M, Dong Y, Xu J, Zhang J, Lv P: Edaravone dexborneol protects cerebral ischemia reperfusion injury through activating Nrf2/HO-1 signaling pathway in mice. Fundam Clin Pharmacol 36:790-800, 2022. https://doi.org/10.1111/fcp.12782

20. Zou Y, Chen Z, Sun C, Yang D, Zhou Z, Peng X, Zheng L, Tang C: Exercise intervention mitigates pathological liver changes in NAFLD zebrafish by activating SIRT1/AMPK/NRF2 signaling. Int J Mol Sci 22:10940, 2021. https://doi.org/10.3390/ijms222010940